

Mat Res Soc Symp. Proc Vol 450, 1987 37 - 376

POLARIZATION INSENSITIVITY IN INTERDIFFUSED, STRAINED InGaAs/InP QUANTUM WELLS

Joseph Micallef, James L. Borg, and Wai-Chee Shiu*

Department of Microelectronics, University of Malta, Msida MSD06, Malta

* Department of Mathematics, Hong Kong Baptist University, Waterloo Road, Hong Kong

ABSTRACT

Theoretical results are presented showing how quantum well disordering affects the TE and TM absorption coefficient spectra of $\text{In}_{0.53}\text{Ga}_{0.47}\text{As}/\text{InP}$ single quantum wells. An error function distribution is used to model the constituent atom composition after interdiffusion. Different interdiffusion rates on the group V and group III sublattices are considered resulting in a strained structure. With a suitable interdiffusion process the heavy hole and light hole ground state, excitonic transition energies merge and the absorption coefficient spectra near the fundamental absorption edge become polarization insensitive. The results also show that this polarization insensitivity can persist with the application of an electric field, which is of considerable interest in waveguide modulators.

INTRODUCTION

There is increasing interest in polarization independent modulators for optical communication systems since optical signals propagating along optical fibres do not usually maintain light polarization. New high-speed applications such as in-line optical pulse reshaping and retiming, and optical demultiplexing [1] require polarization insensitivity. Semiconductor quantum well (QW) optical modulators, which utilize the quantum-confined Stark effect (QCSE), offer the potential of enhanced device performance such as high on/off ratios, low driving voltages, and small device sizes [2,3], and are suitable for monolithic integration with other semiconductor optical devices [4]. However, in waveguide modulators where light propagates parallel to the QW plane, optical absorption exhibits strong polarization dependence since TE polarization interacts mainly with heavy holes while TM polarization interacts with light holes. This polarization sensitivity can be reduced if degeneracy of the heavy- and light-hole exciton peaks is achieved through bandgap engineering.

QW disordering in III-V semiconductors, which results in the interdiffusion of constituent atoms across the well-barrier heterointerfaces, offers the potential of continuous modification of the material bandgap, and hence of varying the absorption edge, in localized areas. The extent of interdiffusion and thus of the bandgap modification can be controlled by the post-growth QW disordering process parameters. This process has been used to produce lateral photon confinement in lasers and optical waveguides [5], shift the emission wavelength of an InP-based quantum well laser structure [6] and it has the potential to improve modulation performance by enhancing the on/off ratio and lowering the drive voltage [7].

Tensile strain in InGaAs/InP QW structures can be used as a tool to obtain polarization independent electroabsorption [8]. Coherent tensile strain reduces the energy gap between the conduction band and both the degenerate valence bands and the spin-orbit split-off band, and

at the same time causes the LH band to move towards the conduction band edge and the HH band to move away from the conduction band edge. One approach that can lead to the merging of the heavy-hole (HH) and light-hole (LH) ground state transition energies is to grow lattice-matched InGaAs/InP QWs and then use post-growth QW interdiffusion to introduce the required tensile strain.

Experimental results of the disordering of $\text{In}_{0.53}\text{Ga}_{0.47}\text{As}/\text{InP}$ QW structures have been interpreted in terms of three different interdiffusion processes. i) comparable interdiffusion rates on both group III and group V sublattices, ii) interdiffusion on group III sublattice only, and iii) interdiffusion on both sublattices but with different interdiffusion rates [9-12]. In this paper the effects of different interdiffusion rates on the two sublattices in an $\text{In}_{0.53}\text{Ga}_{0.47}\text{As}/\text{InP}$ single QW on the fundamental absorption edge for TE and TM polarizations are modelled, taking into consideration the graded compositional profiles and the strain build up that result in the interdiffused QW structure.

COMPUTATIONAL CONSIDERATIONS

An $\text{In}_{0.53}\text{Ga}_{0.47}\text{As}$ layer sandwiched between thick InP barriers is considered here. The interdiffusion processes on the two sublattices are modelled by two different interdiffusion lengths [12]. The interdiffusion of In and Ga atoms is characterized by a diffusion length L_d , which is defined as $L_d = (Dt)^{1/2}$, where D is the diffusion coefficient and t is the diffusion time; the interdiffusion of As and P atoms is characterized by a different diffusion length L'_d . Lattice-matching to InP only exists for $\text{In}_x\text{Ga}_{1-x}\text{As}_y\text{P}_{1-y}$ materials with $y \approx 2.2(1 - x)$ [13], so that for the case being considered here, with $L'_d \neq L_d$, a strained QW structure results. After disordering, the composition of the interdiffused atoms across the QW is assumed to have an error function distribution [14]. The constituent atom compositional profiles can, therefore, be represented as follows:

(i) in the group III sublattice, the In concentration after interdiffusion, $\tilde{x}(z)$, is described by

$$\tilde{x}(z) = 1 - \frac{1-x}{2} \left[\text{erf}\left(\frac{L_z + 2z}{4L_d}\right) + \text{erf}\left(\frac{L_z - 2z}{4L_d}\right) \right]$$

where L_z is the as-grown well width, z is the growth direction, and the QW is centred at $z = 0$.

(ii) in the group V sublattice, the As compositional profile after interdiffusion, $\tilde{y}(z)$, is given by

$$\tilde{y}(z) = \frac{y}{2} \left[\text{erf}\left(\frac{L_z + 2z}{4L'_d}\right) + \text{erf}\left(\frac{L_z - 2z}{4L'_d}\right) \right]$$

where $y = 1$ is the As concentration of the as-grown structure.

The compositional profiles in the disordered QW structure imply that the carrier effective mass, the bulk bandgap, the strain and its effects vary continuously across the QW. Consequently the carrier effective mass, $m_r^*(z)$, is now z -dependent and is obtained from $m_r^*(z) = m_r^*(\tilde{x}, \tilde{y})$ where $m_r^*(x, y)$ is the respective carrier $\text{In}_x\text{Ga}_{1-x}\text{As}_y\text{P}_{1-y}$ bulk effective mass, and r denotes either the electron (C), heavy hole (HH), or light hole (LH). The unstrained (bulk) bandgap in the well $E_g(\tilde{x}, \tilde{y})$, is also a function of the compositional profile, so that the

unstrained potential profile after interdiffusion, $\Delta E_r(\tilde{x}, \tilde{y})$, varies across the well and is given by $\Delta E_r(\tilde{x}, \tilde{y}) = Q_r \Delta E_g(\tilde{x}, \tilde{y})$, where Q_r is the band offset and ΔE_g is the unstrained bandgap offset.

The carrier confinement profile after interdiffusion, obtained by modifying the bulk postprocessing potential profile with the variable strain effects, is determined from [15]

$U_r(z) = Q_r [\Delta E_g(\tilde{x}, \tilde{y}) - S_{\perp}(\tilde{x}, \tilde{y})] \pm S_{\parallel r}(\tilde{x}, \tilde{y})$, where $S_{\perp}(\tilde{x}, \tilde{y})$ is the change in the bulk bandgap due to the biaxial component of strain, and $S_{\parallel r}(\tilde{x}, \tilde{y})$ is the potential corresponding to the HH–LH band edge splitting induced by the uniaxial component of strain. $S_{\parallel \text{HH}}(\tilde{x}, \tilde{y})$ and $S_{\parallel \text{LH}}(\tilde{x}, \tilde{y})$ are asymmetric due to the coupling between the LH and split off band, and $S_{\parallel \text{C}}(\tilde{x}, \tilde{y}) = 0$. The detailed expressions for $S_{\parallel \text{HH}}(\tilde{x}, \tilde{y})$ and $S_{\parallel \text{LH}}(\tilde{x}, \tilde{y})$ are derived in [15].

The electron and hole subband edge structure is obtained using the envelope function scheme by introducing these variations in the appropriate one-electron Schrödinger equation, which is then solved numerically to obtain the subband energy levels, the interband transition energies, and the envelope wave functions. Details of the calculations are given in [15]. The absorption coefficient spectrum near the fundamental absorption edge is next calculated taking into consideration the ground state interband and 1 S exciton optical absorption in the interdiffused structure, where the HH and LH related 1 S exciton binding energies and wave functions are determined by a perturbative-variational method. Details of these calculations are reported in [16]

RESULTS AND DISCUSSION

The structure considered here is an undoped $\text{In}_{0.53}\text{Ga}_{0.47}\text{As}/\text{InP}$ single QW layer, with an as-grown width $L_z = 6$ nm, lattice-matched to thick InP barriers. The interdiffusion process is represented by the condition $L_d' = 2L_d$.

The compositional profile, in-plane strain, and carrier confinement profiles for $L_d' = 2L_d = 1.41$ nm are shown in Fig. 1. The interdiffusion on the group V sublattice is faster than that on the group III sublattice, with the result that the well becomes InGaAsP, Fig. 1(a), with constituent atoms compositional profiles that give rise to a tensile strain in the interdiffused QW, Fig. 1(b). For the structure and interdiffusion conditions considered here a tensile strain of about 0.6% is induced in the centre of the well. The compositional profile also causes a compressive strain in the barrier close to the interface. The combination of the unstrained bandgap and the effects of the strain distribution on this bandgap gives rise to the confinement profiles in Fig. 1(c). The LH potential profile is shifted towards the electron (C) potential profile, while the HH potential profile is shifted away from the electron potential profile. Under these conditions the C–HH and C–LH ground state transition energies coincide. The effects of the tensile strain induced in the interdiffused QW on the HH and LH confinement profiles compensate the energy level splitting of the HH and LH ground states due to the different hole masses.

The TE and TM absorption coefficient spectra near the fundamental absorption edge are shown in Fig. 2, without the application of an electric field and for an applied field $F = 100$ kV/cm. The exciton peaks shift to longer wavelengths with the application of the electric field reflecting the QCSE, and at the same time decrease in value. In the interdiffused QW an enhanced Stark shift can result compared to the as-grown QW [7]. The effective width of the tilted confinement profile experienced by the electron and hole ground states under the action of the applied field is larger in the interdiffused QW than in the as-grown QW. As a result the applied field lowers the ground state subbands, and thus the ground state transition energy to a greater extent in the interdiffused QW. The figure also shows that the fundamental

Fig. 1(a). Composition profile for $L_z = 6$ nm, $L_d' = 1.41$ nm, with well centre at $z = 0$.

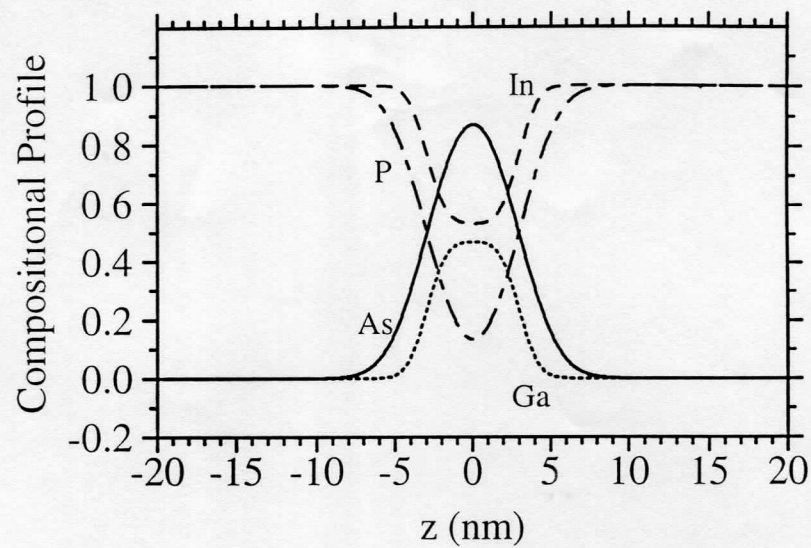


Fig. 1(b). In-plane strain for the interdiffused QW

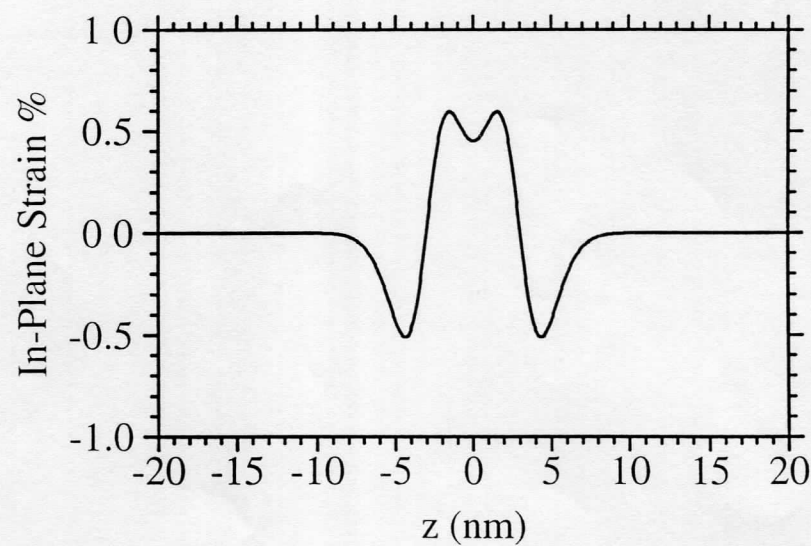
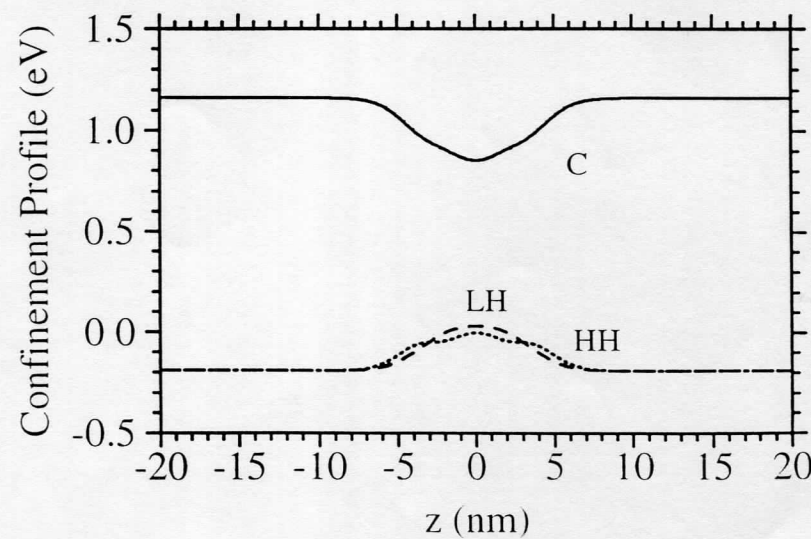


Fig. 1(c) Carrier confinement profiles for electron (C), heavy hole (HH) and light hole (LH).



absorption edges for the two polarizations are quite close to each other for both $F = 0$ and $F = 100$ kV/cm, indicating that polarization insensitive electroabsorption is possible in the interdiffused InGaAsP QW structure.

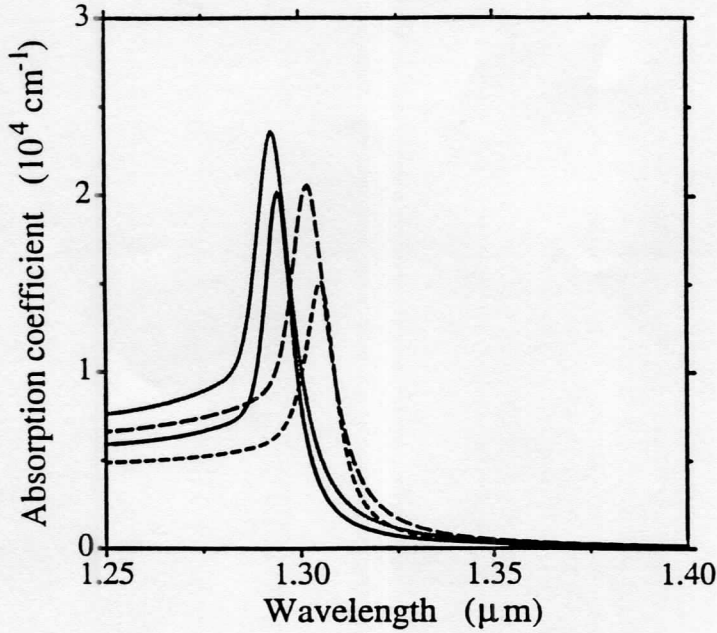


Fig. 2. Absorption coefficient spectra for TE and TM polarization for the interdiffused InGaAs/InP quantum well at $L_d' = 1.41$ nm, calculated for applied electric field $F = 0$ kV/cm, solid line for TE, dotted line for TM, and $F = 100$ kV/cm, short-dash for TE, and long-dash for TM.

Fig. 3 shows the electric field dependence of the absorption coefficient change $\Delta\alpha$ for TE and TM polarizations at the wavelength $\lambda = 1.305 \mu\text{m}$ for the interdiffused QW structure, where $\Delta\alpha = \alpha_F - \alpha_{F=0}$. With the application of an electric field the absorption change increases consistently and a significant increase in $\Delta\alpha$ results at $F = 100$ kV/cm. For the InGaAs/InP QW disordering process parameters considered here, the polarization characteristics of the absorption coefficient change are quite controlled and the polarization insensitivity persists even at the higher electric fields.

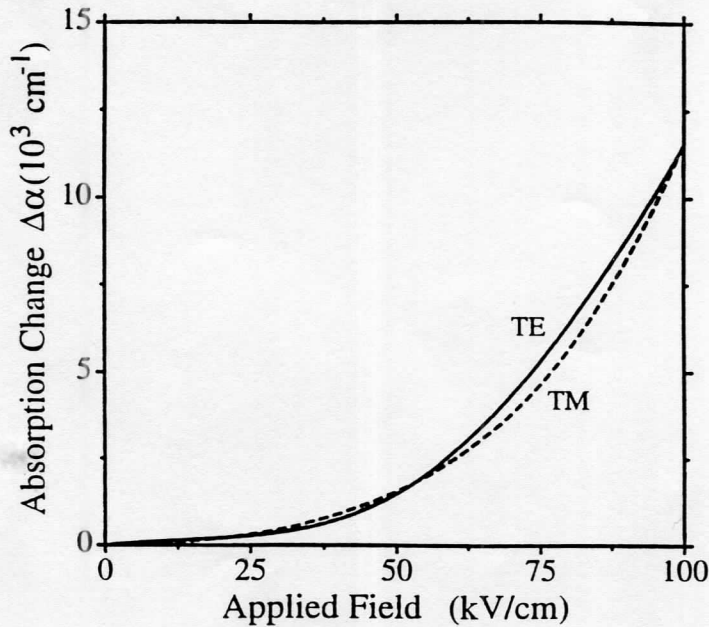


Fig. 3 Absorption coefficient change $\Delta\alpha$ with applied electric field, where $\Delta\alpha = \alpha_F - \alpha_{F=0}$, for TE and TM polarization, for $\lambda = 1.305 \mu\text{m}$

CONCLUSIONS

The interdiffusion of $\text{In}_{0.53}\text{Ga}_{0.47}\text{As}/\text{InP}$ QWs as an approach for controlling the polarization-sensitive characteristics of the absorption coefficient and the absorption change due to the QCSE has been investigated theoretically. When the group V sublattice interdiffusion rate is greater than the group III sublattice interdiffusion rate a tensile strain results in the interdiffused QW, leading to degeneracy of the heavy- and light-hole transition energies. Results presented for absorption coefficient spectra near the fundamental absorption edge, and for the electric field dependence of the absorption coefficient change, indicate that optimization of the interdiffusion process can lead to polarization-insensitive modulation at particular wavelengths. For the QW structure and interdiffusion parameters considered here polarization insensitivity can be achieved around $1.3\ \mu\text{m}$, by inducing a 0.6% tensile strain in the centre of the interdiffused InGaAsP well. This can be a promising approach for polarization-insensitive electroabsorption devices.

ACKNOWLEDGEMENT

This work was supported in part by the RGC Earmarked Research Grant of Hong Kong, and the William Mong Visiting Research Fellowship of the University of Hong Kong.

REFERENCES

1. M. Suzuki, H. Tanaka, N. Edagawa, and Y. Matsushima, *J. Lightwave Technol.* **LT-10**, 1912 (1992).
2. I. Kotaka, K. Wakita, K. Kawano, H. Asai, and M. Naganuma, *Electron. Lett.* **27**, 2162 (1991).
3. T. Ido, H. Sano, D.J. Moss, S. Tanaka, and A. Takai, *IEEE Photon. Technol. Lett.* **6**, 1207, (1994).
4. T.L. Koch, *J. Quantum Electron.* **27**, 641 (1991).
5. W. Xia, S.C. Lin, S.A. Pappert, C.A. Hewett, M. Fernandes, T.T. Vu, P.K.L. Yu, and S.S. Lau, *Appl. Phys. Lett.* **55**, 2020 (1989).
6. P.J. Poole, S. Charbonneau, M. Dion, G.C. Aers, M. Buchanan, R.D. Goldberg, and I.V. Mitchell, *IEEE Photon. Technol. Lett.* **8**, 16 (1996).
7. J. Micallef, E.H. Li, and B.L. Weiss, *Appl. Phys. Lett.* **67**, 2768 (1995).
8. T. Aizawa, K.G. Ravikumar, S. Suzuki, T. Watanabe, and R. Yamauchi, *IEEE J. Quantum Electron.* **30**, 585 (1994).
9. M. Razeghi, O. Archer, and F. Launay, *Semicond. Sci. Technol.* **2**, 793 (1987).
10. I.J. Pape, P. Li Kam Wa, J.P.R. David, P.A. Claxton, P.N. Robson, and D. Sykes, *Electron. Lett.* **24**, 910 (1988).
11. S.A. Schwarz, P. Mei, T. Venkatesen, R. Bhat, D.M. Hwang, C.L. Schwarz, M. Koza, L. Nazar, and B.J. Skromme, *Appl. Phys. Lett.* **53**, 1051 (1988).
12. H. Sumida, H. Asahi, S.J. Yu, K. Asami, S. Gonde, and H. Tanoue, *Appl. Phys. Lett.* **54**, 520 (1989).
13. *GaInAsP Alloy Semiconductors*, ed. T.P. Pearsall, Wiley, New York, 1982, p. 295.
14. T.E. Schlesinger and T. Kuech, *Appl. Phys. Lett.* **49**, 519 (1986).
15. J. Micallef, E.H. Li, and B.L. Weiss, *J. Appl. Phys.* **73**, 7524 (1993).
16. J. Micallef, E.H. Li, and B.L. Weiss, *Superlatt. & Microstructures* **13**, 315 (1993).